

Bioadsorption of Copper(II) Using Halmahera Specific Marine Algae (*Sargassum turbinarioides*) Encapsulated Calcium Alginate

Dede Ardiansyah Takdir Abubakar Sanawi¹, Barlah Rumhayati^{2*}, and Qonitah Fardiyah²

¹Postgraduate Program, Department of Chemistry, Faculty of Mathematics and Natural Sciences, Universitas Brawijaya, Jl. Veteran, Malang 65145, Indonesia

²Department of Chemistry, Faculty of Mathematics and Natural Sciences, Universitas Brawijaya, Jl. Veteran, Malang 65145, Indonesia

* **Corresponding author:**

email: rumhayati_barlah@ub.ac.id

Received: August 11, 2024

Accepted: September 24, 2024

DOI: 10.22146/ijc.99090

Abstract: This study investigated the conditions for bioadsorption of copper(II) using Halmahera marine algae (*Sargassum turbinarioides*) encapsulated with calcium alginate by batch method. Physicochemical parameters of biosorption, including contact time, biosorbent mass, pH, and copper(II) concentration, were studied to determine the percentage of copper(II) adsorbed. The maximum percentage of copper(II) bioadsorption was 96.4% under the optimum bioadsorption conditions with a contact time of 90 min, a biosorbent mass of 2 g, a solution pH of 5, and a copper(II) concentration of 60 mg/L. The bioadsorption isotherm study showed that the Langmuir model is more suitable for modeling copper(II) bioadsorption, while the bioadsorption kinetics study showed a pseudo-second-order kinetic model. Characterization of the biosorbent using FTIR showed that the biosorbent has active functional groups such as O-H, C-H, S-H, C=O, S=O, and C-O-C, which act as metal ligands, and SEM characterization showed morphological changes in the biosorbent before and after the copper(II) bioadsorption process.

Keywords: bioadsorption; copper(II); *S. turbinarioides*; encapsulation; Ca-alginate

■ INTRODUCTION

Environmental pollution continues to increase along with anthropogenic activities, such as the increasing use of heavy metals in industry. These activities result in human health problems and environmental damage. One of the most dangerous impacts of this problem is heavy metal contamination in water [1]. Overwhelming metal contamination within the aquatic environment may be a severe issue, so genuine endeavors are required not to imperil the encompassing life. Some examples of heavy metals that can pollute the environment are copper, arsenic, nickel, zinc, cadmium, mercury, chromium, iron, lead, and aluminum [2-4]. Copper is one of the most common heavy metal contaminants in the environment, as it can result from industrial processes, smelting, mining manufacturing, and refining industries [3]. Copper toxicity can occur due to an excessive increase in the

concentration of metal ions, which can affect health and the surrounding environment. Copper is toxic, has carcinogenic effects, and negatively affects growth, reproduction, and changes in brain function, enzyme activity, and metabolism [5-6].

Copper(II) can be eliminated through various techniques, including ion exchange, membrane filtration, electrochemical processes, and coagulation. Nevertheless, these techniques are characterized by lower efficiency and higher costs, making colloidal particle sludge harmful to the surrounding environment [7]. Efficient and eco-friendly techniques must be devised to eliminate copper(II) from water sources. Using natural materials, such as algae, in adsorption or bioadsorption techniques offers numerous benefits. These methods are environmentally safe and do not pose significant risks or side effects. Moreover, they are highly

efficient in reducing the concentration of metal ions in water [8-9].

The selection of marine algae *Sargassum turbinarioides* as a biosorbent material is due to its vast abundance. The *S. turbinarioides* has various factors that allow it to absorb copper(II) due to the availability of active sites in algae, such as carboxylate and hydroxyl on the algal cell surface [10-11]. These groups can interact with copper(II) through chemical bonding and are responsible for bioadsorption [12]. One disadvantage of algae for metal bioadsorption applications is that they tend to break apart and become difficult to separate from the solution after the bioadsorption process [13]. Thus, it is necessary to increase algae's effectiveness in copper(II) bioadsorption. So, in this study, alginate was added as a matrix to improve the stability of algae as a biosorbent [14-15]. Alginate is a linear, negatively charged polysaccharide that dissolves in water. It is made up of units of β -D-mannuronate (M) and α -L-guluronate (G) linked together in a 1-4 fashion [16]. Alginate readily reacts with divalent cations such as Ca^{2+} to form a firm gel that can hold the material inside for a considerable period. Alginate was chosen because it is non-toxic, readily available, and has many carboxyl groups that provide additional metal binding sites in bioadsorption [17].

This study aimed to utilize biosorbent from Ca-alginate encapsulated marine algae *S. turbinarioides* for copper(II) removal. Bioadsorption of copper(II) was studied at various contact times, biosorbent doses, pH, and copper metal concentrations using a batch method at the laboratory scale. Bioadsorption isotherms and bioadsorption kinetics were also studied.

■ EXPERIMENTAL SECTION

Materials

Samples of marine algae *S. turbinarioides* were from Halmahera, North Maluku waters, with coordinates N $0^{\circ}0'39.23064''$ /E $127^{\circ}24'25.42068''$. The chemicals used in this study were of analytical grade, except as further mentioned. Sodium alginate, calcium chloride (CaCl_2 , $\geq 98\%$), sodium diethyldithiocarbamate ($\text{NaS}_2\text{CN}(\text{C}_2\text{H}_5)_2$, $\geq 98\%$), sodium hydroxide (NaOH , $\geq 98\%$), hydrochloric acid (HCl , $\geq 98\%$), ammonium hydroxide (NH_4OH ,

$\geq 98\%$), and copper stock solution with a concentration of 1000 mg/L made by dissolving copper sulfate pentahydrate ($\text{CuSO}_4 \cdot 5\text{H}_2\text{O}$, $\geq 98\%$) in distilled water.

Instrumentation

The instruments used in this investigation comprised an electronic balance, UV-vis spectrophotometer (Thermo Genesys 10S), oven, magnetic stirrer, and shaker. The biosorbent was characterized before and after bioadsorption using Fourier transforms infrared spectroscopy (FTIR, Shimadzu 8400s) and scanning electron microscope (SEM, Hitachi TM3000).

Procedure

Biosorbent preparation

The preparation of biosorbent from Ca-alginate encapsulated algal biomass of *S. turbinarioides* has been done by modifying the method done by Al-Rub et al. [18] and Barquilha et al. [19]. The biosorbent was prepared by drying the algae in an oven at $60\text{ }^{\circ}\text{C}$ for 20 h, grinding, and sieving with a 100–120 mesh sieve. Biomass that did not pass the 120-mesh sieve was used for biosorbent. *S. turbinarioides* biomass powder was weighted at 1 g, added to 2% w/v sodium alginate, and stirred using a stirrer at 500 rpm for 30 min. The mixture was slowly dispensed into a 4% w/v CaCl_2 solution using a syringe, then left to stand for 1 h to form gel beads. The gel beads were washed with distilled water and then dried using freeze-drying.

Process of bioadsorption

This study conducted the bioadsorption process using the batch method. The experiments involved varying contact times (15, 30, 45, 60, 75, 90, 105, and 120 min), amounts of biosorbent (0.25, 0.5, 0.75, 1, 1.5, 2, and 2.5 g), pH levels of the copper(II) solution (2, 3, 4, 5, and 6), and concentrations of copper(II) (5, 10, 20, 40, 60, 80, and 100 mg L^{-1}). The sample was stirred using a shaker at a velocity of 200 rpm and then separated by filtration to isolate the biosorbent from the copper solution. Furthermore, a UV-vis spectrophotometer assessed the solution's copper concentration before and after the bioadsorption process. The analysis was

performed at 455 nm using a $\text{NaS}_2\text{CN}(\text{C}_2\text{H}_5)_2$ reagent to create a copper(II) complex. The experiments were carried out with three replicates. Eq. (1) and (2) were utilized to calculate the percentage of copper(II) bioadsorption adsorbed (%adsorption) and the quantity of copper(II) adsorbed (q_e);

$$\text{Adsorption (\%)} = \frac{C_i - C_e}{C_i} \times 100\% \quad (1)$$

$$q_e = \frac{C_i - C_e}{W} \times V \quad (2)$$

where q_e = amount of metal ions adsorbed (mg g^{-1}), C_i = initial copper(II) concentration before bioadsorption (mg L^{-1}), C_e = final copper(II) concentration after bioadsorption (mg L^{-1}), V = volume of copper(II) solution (L), and W = biosorbent mass (g).

Bioadsorption isotherm

Bioadsorption isotherms define the state of balance between the adsorbent and the adsorbate [20]. Various theoretical models explain how biosorbents adsorb heavy metals, such as copper. Two of the models included in the group are the Langmuir and Freundlich models. The Langmuir isotherm postulates that sorption occurs at uniform sorption sites on the biosorbent's surface and that bioadsorption occurs in single layers. Conversely, the Freundlich isotherm describes sorption as involving multiple, unevenly distributed layers [21-22].

The linear form of the Langmuir isotherm equation is shown in Eq. (3);

$$\frac{1}{q_e} = \frac{1}{K_L \cdot q_{\max}} \cdot \frac{1}{C_e} + \frac{1}{q_{\max}} \quad (3)$$

where q_e = amount of metal ions adsorbed (mg g^{-1}), C_e = final concentration of copper(II) after bioadsorption (mg L^{-1}), K_L = Langmuir constant, and q_{\max} = maximum bioadsorption capacity or power (L mg^{-1}).

The linear form of the Freundlich isotherm equation can be expressed as in Eq. (4);

$$\log q_e = \log K_F + \frac{1}{n} \log C_e \quad (4)$$

where, q_e = amount of metal ions adsorbed (mg g^{-1}), C_e = final copper(II) concentration after bioadsorption (mg L^{-1}), K_F = Freundlich constant, and n = bioadsorption intensity.

Bioadsorption kinetics

Bioadsorption processes are commonly analyzed using pseudo-first-order and second-order kinetic models to determine their mechanisms. Experimental kinetic data were analyzed using linear regression analysis [21-22]. The pseudo-first-order equation can be expressed in linear form as in Eq. (5);

$$\log(q_e - q_t) = \log q_e - k_1 \cdot t \quad (5)$$

where q_e = amount of copper adsorbed (mg g^{-1}), q_t = amount of copper adsorbed at each time (mg g^{-1}), and k_1 = rate constant (min^{-1}).

The pseudo-second-order equation can be expressed in linear form as in Eq. (6);

$$\frac{t}{q_t} = \frac{1}{k_2 \cdot q_e^2} + \frac{t}{q_e} \quad (6)$$

where q_e = amount of copper adsorbed (mg g^{-1}), q_t = amount of copper adsorbed at each time (mg g^{-1}), and k_2 = equilibrium rate constant of the pseudo-second-order ($\text{g mg}^{-1} \text{min}^{-1}$).

RESULTS AND DISCUSSION

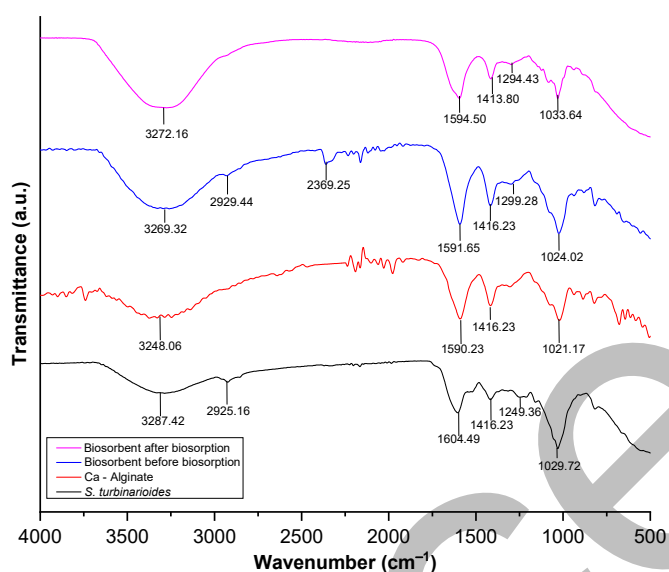
Characterization of Biosorbent

FTIR analysis

FTIR analysis was conducted to identify the active functional groups present in the biosorbent, which are crucial in affecting the bioadsorption process. The results of the FTIR analysis are depicted in Fig. 1, and a comparison of the spectra can be seen in Table 1. The functional groups on the biosorbent before and after bioadsorption show almost the same. FTIR analysis of marine algae powder *S. turbinarioides* showed the presence of hydroxyl (O-H) vibrations at 3287.42 cm^{-1} and identified C-H stretching vibrations at 2925.16 cm^{-1} [23]. The FTIR spectrum of *S. turbinarioides* also showed the presence of carboxylic (C=O) bond at 1604.49 cm^{-1} , a significant component of brown algae [12,24]. The presence of additional peaks such as C-O-C at 1029.72 cm^{-1} and a peak of 1249.36 cm^{-1} which can be attributed to the presence of sulfate (S=O) groups potentially associated with polysaccharides such as fucoidan [11]. The functional groups in the biosorbent have some differences in the peaks produced. The shift

Table 1. Main functional groups present in the sample

Functional group	Wavenumber (cm ⁻¹)			
	<i>S. turbinarioides</i>	Ca-alginate	<i>S. turbinarioides</i> encapsulated Ca-alginate	<i>S. turbinarioides</i> encapsulated Ca-alginate - Cu
O-H	3287.42	3248.06	3260.32	3272.16
C-H	2925.16	-	2929.44	-
S-H	-	-	2369.25	-
C=O	1604.49	1590.23	1591.65	1594.50
C=O	1416.23	1416.23	1416.23	1413.80
S=O	1249.36	-	1299.28	1294.43
C-O-C	1029.72	1021.17	1024.02	1033.64

**Fig 1.** FTIR spectrum of the *S. turbinarioides*, Ca-alginate, biosorbent before, and after bioadsorption

observed at 2360.32 cm^{-1} indicates the stretching vibration of the O-H bond. The peak at 2929.44 cm^{-1} represents the C-H bond stretch, indicating the presence of aliphatic groups. Peaks around 1591.65 and 1416.23 cm^{-1} correspond to asymmetric and symmetric stretching vibrations of the C=O carboxylate in calcium alginate [25]. A new peak appears at 2369.25 cm^{-1} , indicating thiols (S-H) presence. Changes in intensity and wave number of carboxylic groups in pure *S. turbinarioides* and biosorbent (before bioadsorption) can confirm the interaction between marine algae *S. turbinarioides* and Ca-alginate.

Based on FTIR analysis, the biosorbent had active function groups of O-H, C-H, S-H, C=O, S=O, and C-

O-C for bioadsorption. The FTIR analysis sample for the biosorbent after bioadsorption showed that the C-H bond at 2929.44 cm^{-1} and the S-H bond at 2369.25 cm^{-1} disappeared. The peak transmission intensity of the biosorbent after bioadsorption is smaller than that of the biosorbent before bioadsorption. This change is caused by the bioadsorption activity of the analyte on the surface of the biosorbent's active groups.

SEM analysis

SEM analysis has been conducted to study the surface structure of the biosorbent resulting from the interaction with adsorbate. The results of the SEM analysis in Fig. 2 show significant changes in the pore structure of the biosorbent before and after the bioadsorption process with copper(II). Before the bioadsorption process, Fig. 2(a) shows that the biosorbent has open pores. However, after the bioadsorption process, it can be seen that the pore structure has changed. Fig. 2(b) shows the partial closure of the pores and a change in the shape of the pores from open to narrower and closed. These results indicate the sorption of copper(II) ions onto the biosorbent's surface and pores, making the pore structure denser and less open. This change may be due to the accumulation of copper(II) particles within the pores of the biosorbent, blocking access to the pores and changing the surface morphology of the biosorbent [26-27]. The SEM analysis indicates that the copper(II) bioadsorption process significantly affects the pore structure of the biosorbent, which may impact its bioadsorption capacity and efficiency [24,28].

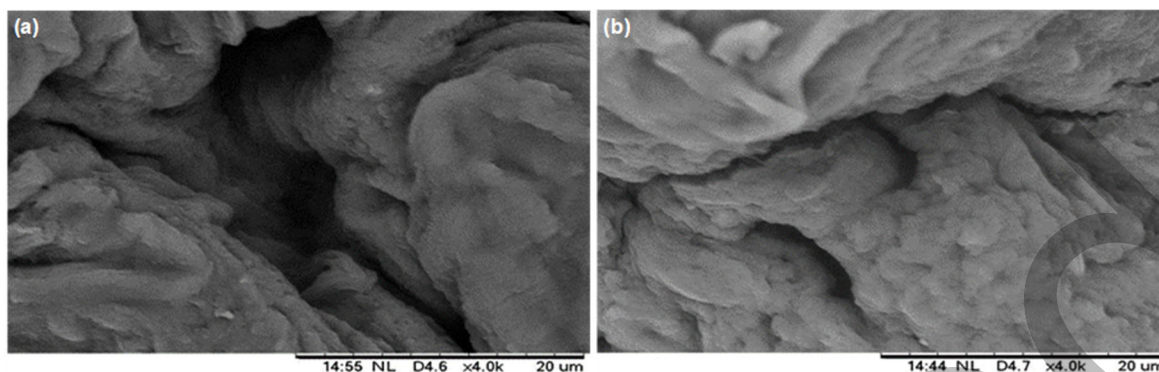


Fig 2. Surface morphology of biosorbent (a) before and (b) after bioadsorption at 4000× magnification

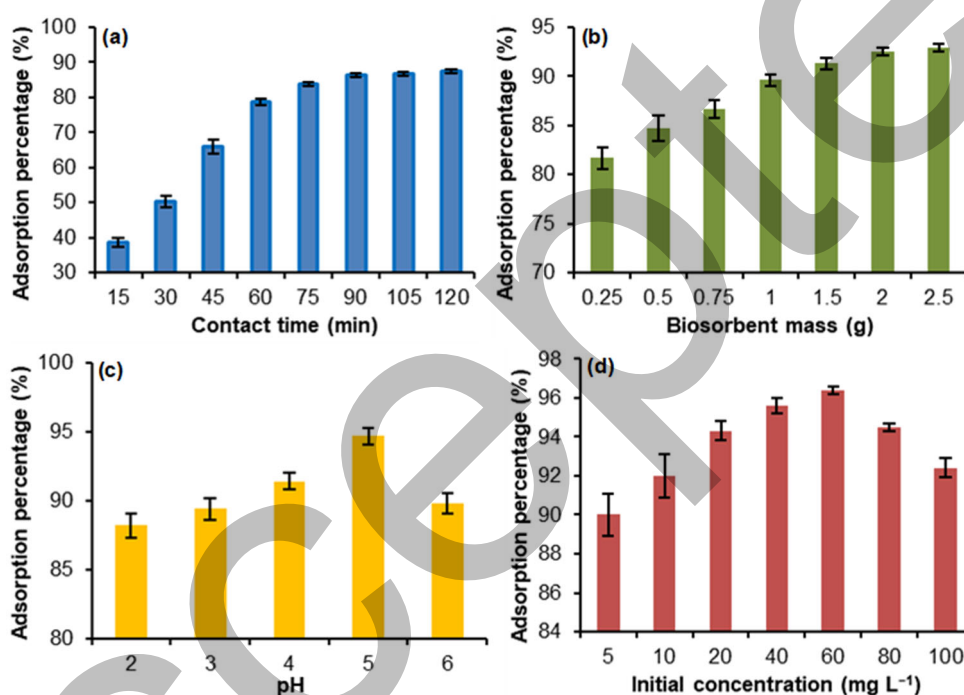


Fig 3. Effect of (a) contact time, (b) biosorbent mass, (c) pH, and (d) initial concentration on the adsorption percentage of copper(II)

Effect of Contact Time

This experiment aimed to ascertain the impact of contact time on the biosorbent's ability to absorb copper(II) until it reaches saturation. Fig. 3(a) shows the correlation between copper(II) adsorption percentage and contact time. The percentage of adsorbed copper(II) bioadsorption tends to increase significantly when the contact starts from 0 to 90 min and starts to slow down until 120 min. The optimum contact time was 90 min with an adsorption percentage of $86.2 \pm 0.7\%$. This follows the theory, which states that the longer the time used, the

more solute can be adsorbed. However, the amount of solute adsorbed will reach a maximum because the surface of the biosorbent has been covered by adsorbed copper(II) ions so that it experiences saturation [12,29]. At the beginning of the adsorption process, increased contact time allows copper(II) ions to interact more with active sites on the biosorbent surface. This usually results in a significant increase in removal percentage in the early stages, as the copper(II) ions quickly interact with active sites on the biosorbent that are not yet saturated. However, as time progresses, the copper(II) removal rate

tends to decrease or remain constant due to the fewer active sites available on the biosorbent [30].

Effect of Biosorbent Mass

The effect of biosorbent mass on copper(II) removal is significant in adsorption. A larger biosorbent mass usually increases the number of active sites available to bind copper(II) ions, thus increasing the total adsorption capacity. The optimum biosorbent mass for copper(II) removal was 2 g with an adsorption percentage of $92.5 \pm 0.5\%$, as shown in Fig. 3(b). With an increase in biosorbent mass, the contact surface area between copper(II) ions and the biosorbent also increases, which allows more ions to be adsorbed [31]. However, a threshold exists where the biosorbent reaches its most effective weight when absorbing metal ions. Any biosorbent weight exceeding this optimal point will reduce metal ion absorption. Additionally, excessive use of biosorbent can lead to particle aggregation, thereby decreasing the usable surface area and complicating the entry of copper(II) ions into the biosorbent's pores [32-33].

Effect of pH

The pH significantly impacts the metal bioadsorption process because it indirectly influences the ionization of metal binding sites on the biosorbent's surface [34]. In the pH range of 2 to 5, the primary form of copper is Cu^{2+} , whereas at pH levels above 6, copper forms insoluble $\text{Cu}(\text{OH})_2$ [35]. Therefore, the formation of $\text{Cu}(\text{OH})_2$ causes the copper metal ions contained in the solution to be less optimally absorbed by the biosorbent. The lowest copper(II) sorption was found at pH 2, as seen in Fig. 3(c). Copper(II) removal then increased and reached a maximum value at pH 5 with an adsorption percentage of $94.7 \pm 0.5\%$. At low pH, H^+ ions will attack positive metal ions to bind to the active site on the negatively charged biosorbent surface. The higher concentration of hydrogen ions will make the biosorbent surface positively charged, which will cause a reduction in the attraction between metal cations and the biosorbent. The biosorbent's carboxyl group ($\text{R}-\text{COOH}$) is the primary ligand responsible for metal sorption at lower pH levels. When the pH is above the range of 1.5–5, the

carboxyl groups in $\text{R}-\text{COOH}$ will undergo deprotonation, generating additional negatively charged bonding sites. Consequently, the biosorbent's ability to absorb metal will be enhanced even more [24,34].

Effect of Metal Ion Concentration

The bioadsorption efficiency of copper(II) is illustrated in Fig. 3(d). As the copper(II) concentration increases from 5 to 60 mg L^{-1} , the copper(II) adsorption percentage rises to $96.4 \pm 0.4\%$. This increase is due to the higher number of metal ions available to interact with the active sites on the biosorbent, which enhances the overall sorption capacity by increasing the likelihood of metal ions binding to the biosorbent surface. However, the adsorption percentage declines when the copper(II) concentration exceeds 60 mg L^{-1} . This reduction occurs because the biosorbent has a limited number of active sites, and at higher concentrations, some copper ions remain un-adsorbed in the solution [36-37]. In addition, the increase in copper(II) concentration allows copper(II) ions to interact more easily with the active sites on the biosorbent, increasing the mass transfer efficiency between the copper(II) ions and the biosorbent. Upon reaching maximum capacity, all active sites on the biosorbent will be occupied by copper(II) ions, causing the biosorbent to become saturated. Although the concentration of copper(II) ions continues to increase, the removal efficiency of copper(II) does not increase significantly [38-39]. Thus, the highest adsorption was observed at a copper(II) concentration of 60 mg L^{-1} , with an adsorption percentage of $96.4 \pm 0.5\%$, indicating that this is the optimal concentration for copper(II) bioadsorption.

Studies on copper(II) adsorption in solution have been conducted with various types of algal biomass. Copper(II) bioadsorption research using *S. angostifolium* biosorbent conducted by Niad et al. [10] revealed that the percentage of adsorbed copper(II) was 58.4% at the optimum condition of the bioadsorption process with a biosorbent mass of 0.4 g, initial concentration of copper(II) 150 mg L^{-1} at pH 6 with a contact time of 60 min at 45°C . Furthermore, Madkour and Dar's [36] research on bioadsorption of copper and zinc with brown algae *Turbinaria turbinata* biosorbent

has a maximum adsorption percentage of 81.07 and 94.0%, respectively. Different types of algae and metals also influence the adsorption percentages [23].

The selection of marine algae as biosorbent materials is due to their natural abundance, which allows them to be utilized effectively as biosorbents. Nevertheless, the primary disadvantage of utilizing pure algae for metal bioadsorption applications lies in their delicate nature, which poses challenges in isolating them from the solution once the bioadsorption process is finished. Thus, there is a need for modification to increase the effectiveness of algae. Petrovič and Simonič [40] have been modifying algae by immobilizing them in Ca-alginate. Immobilization binds algae in a solid matrix of Ca-alginate. Al-Qodah et al. [41] have also modified algae further by phosphorylation. Phosphorylation is a process that aims to generate additional active sites that can react with heavy metals, thereby enhancing the capacity to adsorb them. Table 2 shows the comparison of adsorption percentage with previous studies. Compared to previous studies, the biosorbent derived from Ca-alginate-encapsulated brown marine alga *S. turbinarioides* showed a significant increase in copper adsorption percentage of $96.4 \pm 0.4\%$. Modifying the algae is more effective because it protects them from external conditions and increases stability in the bioadsorption process.

Bioadsorption Isotherm

The bioadsorption behavior of the biosorbent in adsorbing copper(II) was evaluated using Langmuir and Freundlich's isotherm studies. These two models have gained significant popularity due to their simplicity and ability to accurately describe the sorption behavior of copper(II). The Langmuir isotherm graph was derived by plotting $1/q_e$ against $1/C_e$ linearly, while the Freundlich isotherm graph was obtained by plotting $\log q_e$ against $\log C_e$, as depicted in Fig. 4. The bioadsorption data was analyzed using linear regression analysis to compare it with the Langmuir and Freundlich isotherm models. The data in Table 3 reveals that the Langmuir isotherm demonstrates a q_{\max} of 1.02 mg g^{-1} , closely matching the experimental value. Additionally, it exhibits a K_L of 0.22. This outcome suggests that adsorption occurs on a uniform surface with identical activation energy for each adsorbed molecule [41,45].

In contrast, the Freundlich isotherm with a K_F of 2.81 and an n value of 0.88 describes adsorption on heterogeneous surfaces with variations in adsorption energy. This model is more flexible and empirical, suitable for inhomogeneous biosorbent surfaces, and shows varying adsorption efficiency depending on the adsorbate concentration [32]. In conclusion, Langmuir isotherm is better at modeling copper(II) bioadsorption

Table 2. Summarizes studies about copper adsorption using biosorbent from algae

Biosorbent	Optimum condition				Removal (%)	Bioadsorption capacity (mg g^{-1})	Ref
	Contact time (min)	Adsorbent mass (g)	pH	Metal concentration (mg L^{-1})			
<i>S. turbinarioides</i> encapsulated Ca-alginate	90	2.0	5.0	60	96.40	1.48	Present study
<i>Chlorella sorokiniana</i> immobilized Ca-alginate	180	0.3	5.0	50	97.10	37.85	[40]
Spirogyra modification by phosphorylation	160	2.0	6.0	100	74.10	62.60	[41]
<i>Micractinium reisseri</i> immobilized silica	1440	0.2	5.0	10	87.10	1.71	[42]
<i>Sargassum angostifolium</i>	60	0.4	6.0	150	58.40	60.24	[10]
<i>Chlorophyta</i>	60	40.0	4.0	48.3	69.00	12.60	[43]
<i>Turbinaria turbinata</i>	120	1.0	4.5	5	81.07	0.40	[36]
<i>Halimeda opuntia</i>	120	1.0	4.5	15	96.80	1.45	[36]
<i>Gracilaria changii</i>	60	0.3	6.0	5	47.00	0.70	[44]
<i>Cystoseira indica</i>	1440	0.6	4.0	125	35.00	72.10	[45]

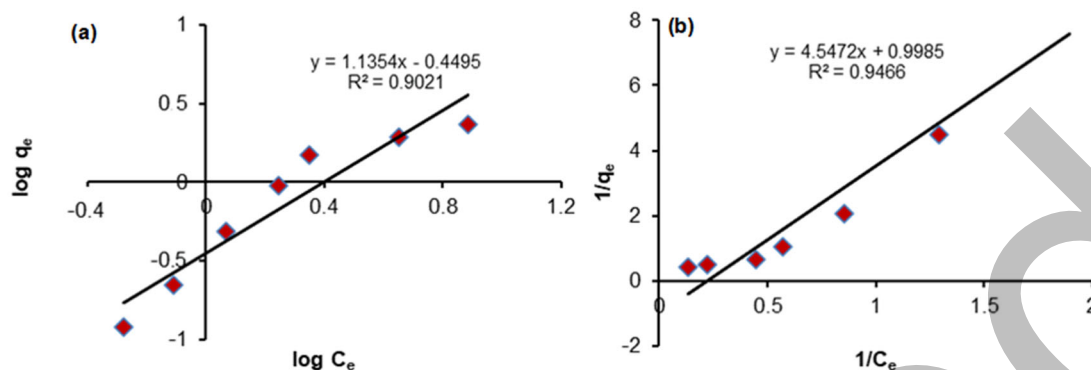


Fig 4. Isotherm plots for bioadsorption (a) Langmuir and (b) Freundlich isotherm models

Table 3. Isotherm model parameter values

q_e exp	Langmuir			Freundlich		
	q_{max}	K_L	R^2	K_F	N	R^2
1.48	1.02	0.22	0.946	2.81	0.88	0.902

using biosorbent algae *S. turbinarioides* encapsulated in Ca-alginate with an R^2 value of 0.9466. These results also indicate that bioadsorption occurs in a monolayer on a homogeneous surface with a chemisorption mechanism, where there is a chemical interaction between copper(II) and active sites on the biosorbent surface.

Bioadsorption Kinetic

Kinetic models are fundamental in determining the affinity or capacity of biosorbents in adsorbing metals. This study used two kinetic models, pseudo-first-order

and pseudo-second-order, to describe the copper(II) bioadsorption process. Fig. 5 shows a linear graph of $\ln(q_e - q_t)$ versus contact time for the pseudo-first-order model and t/q_t versus contact time for the pseudo-second-order model. The analysis results can be seen in Table 4, which shows that the pseudo-second-order model fits the experimental data better than the pseudo-first-order model. This is indicated by the higher R^2 value (0.961) in the pseudo-second-order model compared to the pseudo-first-order model (0.931), indicating that the bioadsorption process follows more pseudo-second-order kinetics. The calculated equilibrium adsorption capacity q_e for the pseudo-second-order model was 1.78 mg g^{-1} with a rate constant k_2 of $0.5615 \text{ g mg}^{-1} \text{ min}^{-1}$. In contrast, in the pseudo-first-order model, q_e was 2.41 mg g^{-1} with

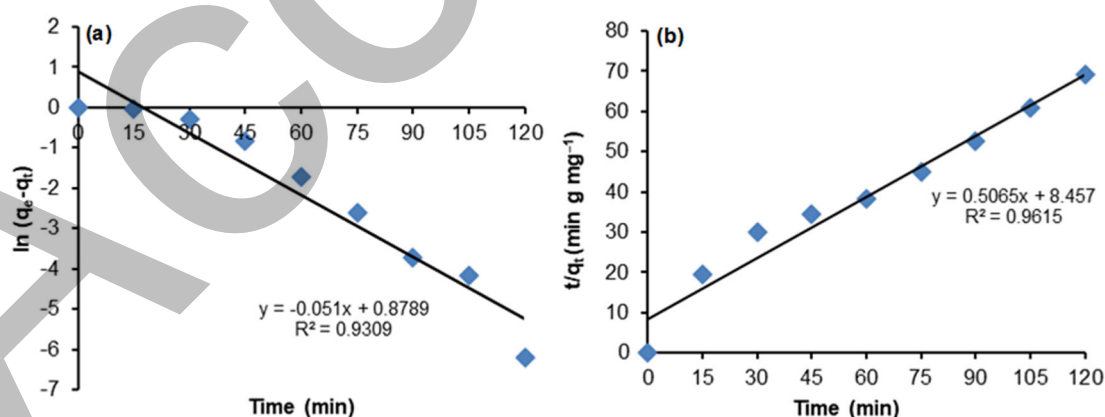


Fig 5. Kinetics plot for copper (II) bioadsorption of (a) pseudo-first-order and (b) pseudo-second-order

Table 4. Kinetics model parameter values

Pseudo-first-order			Pseudo-second-order		
q_e (mg g^{-1})	k_1 (min^{-1})	R^2	q_e (mg g^{-1})	k_2 ($\text{g mg}^{-1} \text{ min}^{-1}$)	R^2
2.41	4.3×10^{-4}	0.931	1.78	0.5615	0.961

a k_1 of $4.3 \times 10^{-4} \text{ min}^{-1}$. Although the q_e value in the pseudo-first-order model is higher, the fit of the experimental data with the pseudo-second-order model is better. This study concludes that the kinetics of the copper(II) bioadsorption process is mainly determined by the chemical reaction speed between the sorbent and the sorbate, indicating that the dominant bioadsorption mechanism is chemisorption [43].

■ CONCLUSION

Based on the results obtained, this study demonstrates that copper(II) biosorption using *S. turbinarioides* biosorbent encapsulated with Ca-alginate is effective in copper(II) biosorption. The maximum adsorption percentage achieved was $96.4 \pm 0.4\%$ under the conditions of 90 min contact time, 2 g biosorbent mass, solution pH 5, and an initial copper(II) concentration of 60 mg L^{-1} , with a biosorption capacity of $1.48 \pm 0.1 \text{ mg g}^{-1}$. These physicochemical parameters are crucial in facilitating the interaction between copper ions and the functional groups in the biosorbent, leading to effective metal ion removal. Furthermore, the biosorption of copper(II) in this study followed the Langmuir isotherm model and the pseudo-second-order kinetic model, with a q_{max} of 1.02 mg g^{-1} , a K_L of 0.22, and a k_2 of $0.5615 \text{ g mg}^{-1} \text{ min}^{-1}$. The results confirm that algae *S. turbinarioides* encapsulated with Ca-alginate is a good alternative for effectively removing copper(II) from water.

■ ACKNOWLEDGMENTS

The authors would like to thank the research financial funding under the scheme of *Penelitian Tesis Magister* with contract number of 00309.37/UN10.A0501/B/PT.01.03.2/2024.

■ CONFLICT OF INTEREST

The authors have no conflict of interest.

■ AUTHOR CONTRIBUTIONS

All authors contributed to the study's preparation and design. The research assistant, Dede Ardiansyah, was responsible for the execution of the experiments, the data analysis, and the article's composition. The experiments were supervised, the data was analyzed, and the

manuscript was revised by Barlah Rumhayati, the research team's leader. Qonitah Fardiyah is a research team member who analyzed the data and offered recommendations for the study. The data analysis and manuscript improvement were the joint efforts of all authors.

■ REFERENCES

- [1] Arif, A., Malik, M.F., Liaqat, S., Aslam, A., Mumtaz, K., Afzal, A., Mahmood Ch, D., Nisa, K., Khursid, F., Arif, F., Khalid, M.S.Z., and Javed, R., 2020, Water pollution and industries, *Pure Appl. Biol.*, 9 (4), 2214–2224.
- [2] Budianta, W., 2021, Heavy metal pollution and mobility of sediment in Tajum River caused by artisanal gold mining in Banyumas, Central Java, Indonesia, *Environ. Sci. Pollut. Res.*, 28 (7), 8585–8593.
- [3] Yusfaddillah, A., Dwi Saputri, R., Edelwis, T.W., and Pardi, H., 2023, Heavy metal pollution in Indonesian waters, *BIO Web Conf.*, 79, 04001.
- [4] Hamuna, B., and Tanjung, R.H.R., 2021, Heavy metal content and spatial distribution to determine the water pollution index in Depapre waters, Papua, Indonesia, *Curr. Appl. Sci. Technol.*, 21 (1), 1–11.
- [5] Valko, M., Morris, H., and Cronin, M.T.D., 2005, Metals, toxicity and oxidative stress, *Curr. Med. Chem.*, 12 (10), 1161–1208.
- [6] Mesquita, A.F., Gonçalves, F.J.M., and Gonçalves, A.M.M., 2023, The lethal and sub-lethal effects of fluorinated and copper-based pesticides—A review, *Int. J. Environ. Res. Public Health*, 20 (4), 1–22.
- [7] Liu, Y., Wang, H., Cui, Y., dan Chen, N., 2023, Removal of copper ions from wastewater: A review, *Int. J. Environ. Res. Public Health*, 20 (5), 3706.
- [8] Znad, H., Awual, M.R., and Martini, S., 2022, The utilization of algae and seaweed biomass for bioremediation of heavy metal contaminated wastewater, *Molecules*, 27 (4), 1275.
- [9] Jeremias, J.S.D., Lin, J.Y., Dalida, M.L.P., and Lu, M.C., 2023, Abatement technologies for copper containing industrial wastewater effluents - A review, *J. Environ. Chem. Eng.*, 11 (2), 109336.

- [10] Niad, M., Rasoolzadeh, L., and Zarei, F., 2014, Biosorption of copper(II) on *Sargassum angostifolium* C. agardh phaeophyceae biomass, *Chem. Speciation Bioavailability*, 26 (3), 176–183.
- [11] Artemisia, R., Setyowati, E.P., Martien, R., and Nugroho, A.K., 2019, The properties of brown marine algae *Sargassum turbinarioides* and *Sargassum ilicifolium* collected from Yogyakarta, Indonesia, *Indones. J. Pharm.*, 30 (1), 43–51.
- [12] Saldarriaga-Hernandez, S., Nájera-Martínez, E.F., Martínez-Prado, M.A., and Melchor-Martínez, E.M., 2020, *Sargassum* based potential biosorbent to tackle pollution in aqueous ecosystems – An overview, *Case Stud. Chem. Environ. Eng.*, 2, 100032.
- [13] Bilal, M., Rasheed, T., Sosa-Hernández, J.E., Raza, A., Nabeel, F., and Iqbal, H.M.N., 2018, Biosorption: An interplay between marine algae and potentially toxic elements—A review, *Mar. Drugs*, 16 (2), 65.
- [14] de Souza Coração, A.C., dos Santos, F.S., Duarte, J.A., Lopes-Filho, E.A.P., De-Paula, J.C., Rocha, L.M., Krepsky, N., Fiaux, S.B., and Teixeira, V.L., 2020, What do we know about the utilization of the *Sargassum* species as biosorbents of trace metals in Brazil?, *J. Environ. Chem. Eng.*, 8 (4), 103941.
- [15] Solo, A.A., Rumhayati, B., and Masruri, M., 2023, Hardness water removal by using cellulose papyrus fibers (*Borrassus flabelifer* L) from East Nusa Tenggara modified with citric acid, *Media Konservasi*, 28 (2), 129–134.
- [16] Najafi-Soulari, S., Shekarchizadeh, H., and Kadivar, M., 2016, Encapsulation optimization of lemon balm antioxidants in calcium alginate hydrogels, *J. Biomater. Sci., Polym. Ed.*, 27 (16), 1631–1644.
- [17] Shalapy, A., Zhao, S., Zhang, C., Li, Y., Geng, H., Ullah, S., Wang, G., Huang, S., and Liu, Y., 2020, Adsorption of deoxynivalenol (DON) from corn steep liquor (CSL) by the microsphere adsorbent SA/CMC loaded with calcium, *Toxins*, 12 (4), 208.
- [18] Abu Al-Rub, F.A., El-Naas, M.H., Benyahia, F., and Ashour, I., 2004, Biosorption of nickel on blank alginate beads, free and immobilized algal cells, *Process Biochem.*, 39 (11), 1767–1773.
- [19] Barquilha, C.E.R., Cossich, E.S., Tavares, C.R.G., and Silva, E.A., 2019, Biosorption of nickel(II) and copper(II) ions by *Sargassum* sp. in nature and alginate extraction products, *Bioresour. Technol. Rep.*, 5, 43–50.
- [20] Rusdiyana, D.N.A., Purnamawati, A.E., Astuti, D.H., and Sani, S., 2023, Penentuan persamaan Langmuir dan Freundlich pada adsorpsi logam Cu(II) air limbah elektroplating dengan silika dari abu vulkanik gunung Bromo, *Inovasi Teknik Kimia*, 8 (2), 83–88.
- [21] Hansen, H.K., Gutiérrez, C., Valencia, N., Gotschlich, C., Lazo, A., Lazo, P., and Ortiz-Soto, R., 2023, Selection of operation conditions for a batch brown seaweed biosorption system for removal of copper from aqueous solutions, *Metals*, 13 (6), 1008.
- [22] Ni'am, A.C., Suhar, M., and Fenelon, E., 2023, Characterization and potential of *Samanea saman*-activated carbon on adsorption of copper from an aqueous solution, *Adsorpt. Sci. Technol.*, 2023, 1911596.
- [23] Jayakumar, V., Govindaradjane, S., Rajamohan, N., and Rajasimman, M., 2022, Biosorption potential of brown algae, *Sargassum polycystum*, for the removal of toxic metals, cadmium and zinc, *Environ. Sci. Pollut. Res.*, 29 (28), 41909–41922.
- [24] Osman, N.S., Md Ali, U.F., Gopinath, S.C.B., Hussin, F., and Aroua, M.K., 2024, Bio-removal of lead(II) ions under optimal condition by zinc chloride-impregnated activated carbon from brown alga, *Biomass Convers. Biorefin.*, s13399-024-05404-9.
- [25] Nastaj, J., Przewłocka, A., and Rajkowska-Myśliwiec, M., 2016, Biosorption of Ni(II), Pb(II) and Zn(II) on calcium alginate beads: Equilibrium, kinetic and mechanism studies, *Pol. J. Chem. Technol.*, 18 (3), 81–87.
- [26] Dulla, J.B., Tamana, M.R., Boddu, S., Pulipati, K., and Srirama, K., 2020, Biosorption of copper(II) onto spent biomass of *Gelidiella acerosa* (brown marine algae): Optimization and kinetic studies, *Appl. Water Sci.*, 10 (2), 56.

- [27] González Fernández, L.A., Navarro Frómeta, A.E., Carranza Álvarez, C., Flores Ramírez, R., Díaz Flores, P.E., Castillo Ramos, V., Sánchez Polo, M., Carrasco Marín, F., and Medellín Castillo, N.A., 2023, Valorization of *Sargassum* biomass as potential material for the remediation of heavy-metals-contaminated waters, *Int. J. Environ. Res. Public Health*, 20 (3), 2559.
- [28] El-Sheekh, M., El-Sabagh, S., Abou Elsoud, G., and Elbeltagy, A., 2020, Efficacy of immobilized biomass of the seaweeds *Ulva lactuca* and *Ulva fasciata* for cadmium biosorption, *Iran. J. Sci. Technol., Trans. A: Sci.*, 44 (1), 37–49.
- [29] Akbari, M., Hallajisani, A., Keshtkar, A.R., Shahbeig, H., and Ali Ghorbanian, S., 2015, Equilibrium and kinetic study and modeling of Cu(II) and Co(II) synergistic biosorption from Cu(II)-Co(II) single and binary mixtures on brown algae *C. indica*, *J. Environ. Chem. Eng.*, 3 (1), 140–149.
- [30] Kang, J.K., Pham, B.N., Lee, C.G., and Park, S.J., 2023, Biosorption of Cd^{2+} , Cu^{2+} , Ni^{2+} , Pb^{2+} by four different macroalgae species (*Costaria costata*, *Hizikia fusiformis*, *Gracilaria verrucosa*, and *Codium fragile*), *Int. J. Environ. Sci. Technol.*, 20 (9), 10113–10122.
- [31] Afroze, S., and Sen, T.K., 2018, A review on heavy metal ions and dye adsorption from water by agricultural solid waste adsorbents, *Water, Air, Soil Pollut.*, 229 (7), 225.
- [32] Foroutan, R., Esmaeili, H., Abbasi, M., Rezakazemi, M., and Mesbah, M., 2018, Adsorption behavior of Cu(II) and Co(II) using chemically modified marine algae, *Environ. Technol.*, 39 (21), 2792–2800.
- [33] Mahmood, Z., Zahra, S., Iqbal, M., Raza, M.A., and Nasir, S., 2017, Comparative study of natural and modified biomass of *Sargassum* sp. for removal of Cd^{2+} and Zn^{2+} from wastewater, *Appl. Water Sci.*, 7 (7), 3469–3481.
- [34] Ibrahim, W.M., Hassan, A.F., and Azab, Y.A., 2016, Biosorption of toxic heavy metals from aqueous solution by *Ulva lactuca* activated carbon, *Egypt. J. Basic Appl. Sci.*, 3 (3), 241–249.
- [35] Cuppett, J.D., Duncan, S.E., and Dietrich, A.M., 2006, Evaluation of copper speciation and water quality factors that affect aqueous copper tasting response, *Chem. Senses*, 31 (7), 689–697.
- [36] Madkour, A.G., and Dar, M.A., 2021, Biosorption of Cu and Zn in a batch system via dried macroalgae *halimeda opuntia* and *turbinaria turbinata*, *Environ. Res. Eng. Manage.*, 77 (1), 76–84.
- [37] Lekshmi, R., Rejiniemon, T.S., Sathya, R., Kuppusamy, P., AL-mekhlafi, F.A., Wadaan, M.A., and Rajendran, P., 2022, Adsorption of heavy metals from the aqueous solution using activated biomass from *Ulva flexuosa*, *Chemosphere*, 306, 135479.
- [38] Saldarriaga-Hernandez, S., Hernandez-Vargas, G., Iqbal, H.M.N., Barceló, D., and Parra-Saldívar, R., 2020, Bioremediation potential of *Sargassum* sp. biomass to tackle pollution in coastal ecosystems: Circular economy approach, *Sci. Total Environ.*, 715, 136978.
- [39] Raju, C.A.I., Anitha, J., Mahalakshmi Kalyani, R., Satyanandam, K., and Jagadeesh, P., 2021, Sorption of cobalt using marine macro seaweed *graciliariacorticata* red algae powder, *Mater. Today: Proc.*, 44, 1816–1827.
- [40] Petrovič, A., and Simonič, M., 2016, Removal of heavy metal ions from drinking water by alginate-immobilised *Chlorella sorokiniana*, *Int. J. Environ. Sci. Technol.*, 13 (7), 1761–1780.
- [41] Al-Qodah, Z., Al-Shannag, M., Amro, A., Assirey, E., Bob, M., Bani-Melhem, K., and Alkasrawi, M., 2017, Impact of surface modification of green algal biomass by phosphorylation on the removal of copper(II) ions from water, *Turk. J. Chem.*, 41 (2), 190–208.
- [42] Lee, H., Shim, E., Yun, H.S., Park, Y.T., Kim, D., Ji, M.K., Kim, C.K., Shin, W.S., and Choi, J., 2016, Biosorption of Cu(II) by immobilized microalgae using silica: Kinetic, equilibrium, and thermodynamic study, *Environ. Sci. Pollut. Res.*, 23 (2), 1025–1034.
- [43] Cygnarowska, K., 2023, The use of algae to remove copper and lead from industrial wastewater, *Geol. Geophys. Environ.*, 49 (1), 85–93.

- [44] Lavania-Baloo, Idayu, N., Salihi, I.U., dan Zainoddin, J., 2017, The use of macroalgae (*Gracilaria changii*) as bio-adsorbent for copper(II) removal, *IOP Conf. Ser.: Mater. Sci. Eng.*, 201 (1), 012031.
- [45] Roozegar, M., and Behnam, S., 2019, An eco-friendly approach for copper(II) biosorption on alga *Cystoseira indica* and its characterization, *Environ. Prog. Sustainable Energy*, 38 (s1), S323–S330.